

## ANOMALIES OF JOULE HEAT, THERMAL AND TURBULENT FLOW FIELDS IN CLOGGED INDUSTRIAL CHANNEL INDUCTION FURNACES

S. Pavlovs<sup>(1)</sup>, A. Jakovics<sup>(1)</sup>, D. Bosnyaks<sup>(1)</sup>, B. Nacke<sup>(2)</sup>, E. Baake<sup>(2)</sup>

<sup>(1)</sup>Laboratory for Mathematical Modelling of Environmental and Technological Processes, University of Latvia, 8 Zellu str., LV-1002, Riga, Latvia

<sup>(2)</sup>Institute of Electrotechnology, Leibniz University of Hannover, Wilhelm-Busch-Str. 4, D-30167 Hannover, Germany

**ABSTRACT.** The computations of industrial channel induction furnace (CIF) have been performed for several typical shapes of clogging, which are the result of CIF long-term operation. The model with extremely build-up of zone of channel outlet to throat and the model with sediments of throat bottom are considered. Appeared due to non-conductive sediments the anomalies in distributions of induced *Joule* heat power, temperature, velocity and turbulent kinetic energy (TKE) are obtained with sequence application of Shear Stress Transport (SST)  $k-\omega$  and Large Eddy Simulation (LES) models of turbulence. Obtained for clogged CIFs physical fields' distributions show noticeable distinctions of its characteristic parameters from non-clogged CIF. The anomalies may negatively influence on CIF operation.

### INTRODUCTION

CIF, popular industrial metallurgical MHD equipment with high electrical and thermal efficiency, is used for melting, holding and casting of metals and alloys. Damages like erosion, clogging and infiltration of the ceramic lining in the channel as well as local overheating in the channel may lower the cleanness of the processed melt as well as the effectiveness and safety of CIF operation. The way to minimize these known problems is the variation of CIF parameters and choice of CIF operation regimes, which provide controlled intensification of turbulent heat exchange between the channel and the throat.

Several types of CIF clogging, which may influence on CIF operation parameters, have been discussed in [1,2]. The current paper presents the further development of CIF numerical modelling of clogged CIFs [5], based on authors' experience of non-clogged CIF long-term computations [3-5].

### CONSIDERED CIF MODELS

The base model for comparison of computational results, which are obtained for clogged CIF, is model with symmetrical channel branches (named '*non-clogged model*'), developed and widely presented in previous author's papers – see for example [3, Figure 1].

For sequent SST and LES computations of influence of non-conductive sediments on *Joule* heat, velocity, temperature and TKE fields the following CIF models are chosen:

- The model (named '*clogged throat model*'), represented in Figures 1(a), 2(a), simulates CIF with sediments at the throat bottom in form of "hill".
- The model (named '*build-up channel model*'), shown in Figures 1(b), 2(b), with narrowed left channel branch, which has 25% of cross-sectional area of right channel branch, simulates build-up in CIF channel.

Note, that chosen models represent the generalized shapes of sediments and built-up, which may be found experimentally in clogged industrial CIFs after long-term operation

[1,2]. As computed flow time period (~1 minute) is more than for five orders smaller than industrial CIFs operation time (~6 months) it is supposed that the shapes of sediments and built-up in chosen models don't change during physical fields modelling. One more assumption is that heat transfer coefficients at surfaces with build-up and sediments are the same to corresponding values in non-clogged model.

The amplitude value of inductor current (total number of turns – 28) is chosen equal for all models – 1850 A. The main computed integral parameters of models are collected in Table 1.

Table 1. Characteristic parameters of computed models

	Clogged throat model	Build-up channel model	Non-clogged model
<i>Joule</i> heat power			
• integral (kW)	250	223	215
• maximum value ( $W/m^3$ )	$1.9 \cdot 10^7$	$6.7 \cdot 10^7$	$1.74 \cdot 10^7$
• position of maximum	throat bottom at sediments base	narrowed zone of left channel branch	channel loop zone facing yoke
Time-averaged temperature (K):			
• maximum value in the channel	~1864	~1832	~1805
• overheating temperature	~48	~37	~32
Velocity (m/s)			
• instantaneous velocity's maximum in clogging zone	~1.8	~3.0	~1.7 (channel outlet)
• fluctuations in time of transit velocity (x-component of velocity area-averaged for cross-section $x=0$ )	from -0.066 till 0.021	from -0.075 till 0.093	from -0.097 till 0.092
• time-averaged value of transit velocity	-0.020	-0.009	-0.028

### PEQUILARITIES OF COMPUTATIONS

Electromagnetic (EM) field, including *Lorentz* force and *Joule* heat, the sources for further flow and temperature modelling, is computed by ANSYS 14.0 for channel and throat with sediments, inductor and iron yoke geometries shown in Figures 1(a) and 1(b). The generated mesh, which takes into account EM field skin-layer, consists of 0.8–1.5 millions of elements.

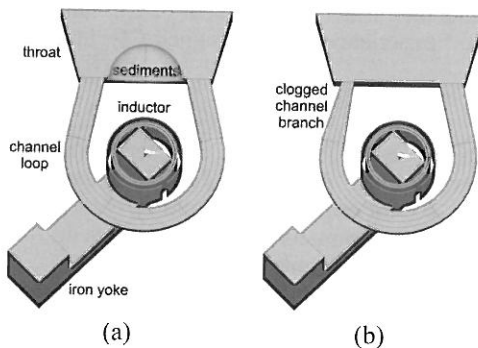


Figure 1. CIF models for EM computations:  
 (a) clogging of throat bottom in form of "hill";  
 (b) narrowed (25%) left channel branch

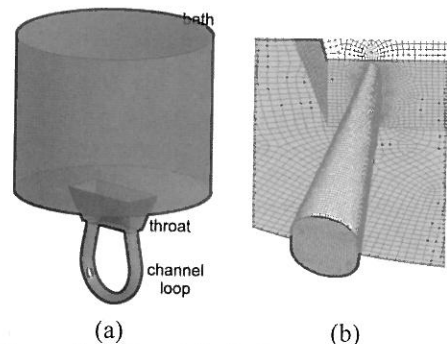


Figure 2. CIF models for HD computations:  
 (a) clogged throat – Figure 1(a);  
 (b) mesh for narrowed (25%) left channel branch in outlet zone to throat – Figure 1(b)

The numerical computations of turbulent hydrodynamic (HD) and thermal fields have been performed using ANSYS CFX 14.0 package with consequent application of transient SST  $k-\omega$  model of turbulence and LES approach. The reached flow time periods are the following:

- for *clogged throat model* total flow time is 41 sec, including 27 sec computed with SST and 14 sec obtained with LES – results for both models are shown in Figure 4;
- for *build-up channel model* total flow time is 88 sec, which consists of 60 sec obtained with SST as well as period of 28 sec computed with LES, which shown in Figure 6.

Note that mentioned durations of computed flow periods are not enough for long-term analysis of possible low frequency oscillation, similar to results obtained during previous research of channel and iron yoke geometries, based on CIF original design [5].

The structured mesh for HD and thermal field modelling (Figure 2(b)), which consists of up to 3.5 millions of elements, takes into account the contradictory requirements in multi-zone CIF model, including variable transversal cross-section of the channel and boundary layers at all solid wall and cooling surfaces with further control of distribution of wall function  $y^+$  at all solid walls (usually  $y^+ < 200-300$ ).

The choice of time step (usually 0.005 sec for SST  $k-\omega$  and 0.0025 sec for LES) on the frontier of computational process stability needs special control of *Courant* number in zone of flow from extremely narrowed left outlet to throat with high velocity values (Figures 3), which appear due to melt incompressibility condition – it demands conservation of integral rate of flow through any pair of channel's transversal cross-sections.

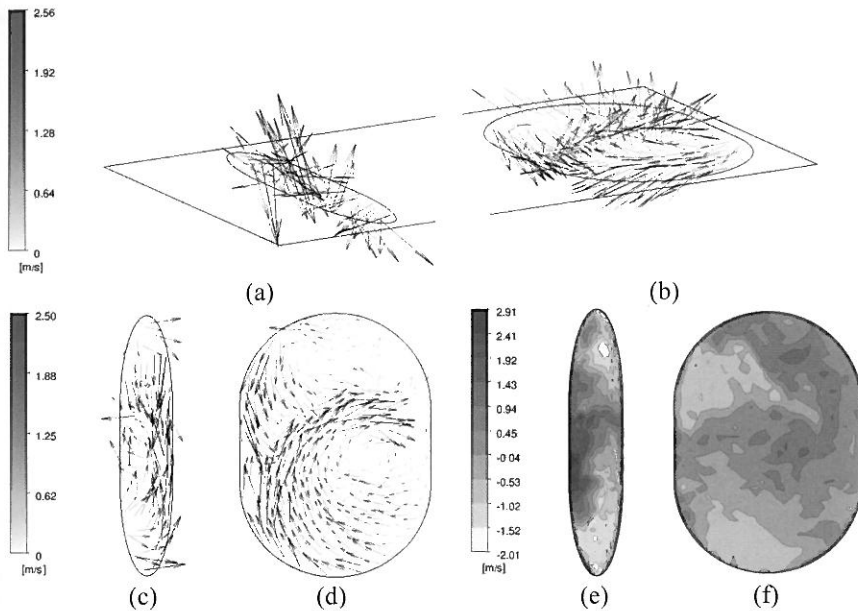


Figure 3. CIF with narrowed (25%) channel branch – Figure 1(b).

Instantaneous velocity at cross-sections  $z = 0.394$  m of left narrowed (a,c,e) and right (b,d,f) channel branches' outlets to throat:

$$(a,b) \ v_x \bar{e}_x + v_y \bar{e}_y + v_z \bar{e}_z; (c,d) \ v_x \bar{e}_x + v_y \bar{e}_y; (e,f) \ v_z$$

It is essentially to mention for engineering application, that at present the computations of industrial CIF models may be performed using mainstream desktop workstation equipped with single 4-core (8-thread) 64-bit processor. The estimated computation time (processor clock frequency up to 3.5 GHz) is 5–7 days to obtain 1 sec of flow time.

## ANOMALIES OF PHYSICAL FIELDS IN CLOGGED THROAT MODEL

The changes of CIF geometry due to non-conductive sediments in clogged bottom of throat are the cause of noticeable concentration of *Joule* heat density

$$Q = \frac{J^2}{2\sigma} \quad (1)$$

at the bottom of the interface of sediments and slant surface of throat (Figure 5(d)) due to drastic decrease of transversal cross-section of induced current loop and sequent increase of its current density  $J$ . The maximum value of the *Joule* heat density  $1.9 \cdot 10^7 \text{ W/m}^3$  is for  $\approx 10\%$  greater than maximum value  $1.72 \cdot 10^7 \text{ W/m}^3$  at bottom of inner surface of channel loop (Figure 5(a)). For non-clogged CIF the maximum values of *Joule* heat in channel loop and in throat bottom are accordingly  $1.74 \cdot 10^7 \text{ W/m}^3$  and  $0.9 \cdot 10^7 \text{ W/m}^3$  [5].

In spite of *Joule* heat anomaly the temperature field at vertical cross-section  $y=0$  (Figure 5(b)) has the similar qualitative distribution as in non-clogged CIF [3,4]. The changes of maximum value of instantaneous temperature in dependence of flow time are shown in Figure 4. Note, than application of LES approach provides more detailed information of both instantaneous and time-averaged  $T_{\max}$  and its position in the channel loop in comparison with two-parameter SST  $k-\omega$  model of turbulence.

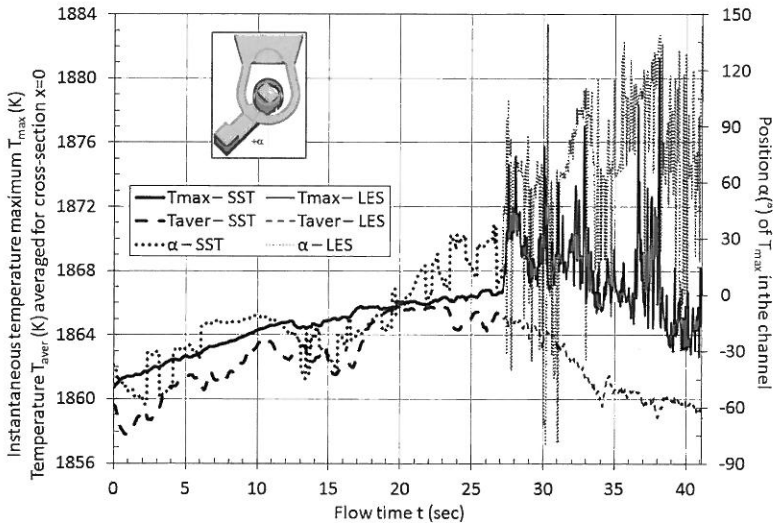


Figure 4. CIF with clogged throat – Figure 1(a).

Maximum of instantaneous temperature  $T_{\max}$  (K) and angle  $\alpha$  ( $^\circ$ ) of its position at cross-section  $y = 0$ ; averaged for cross-section  $x=0$  (bottom of channel loop) temperature  $T_{\text{aver}}$  (K) – for flow time periods and with models of turbulence:  $t = 0-27$  sec with  $k-\omega$  SST and  $t = 27-41$  sec with LES

Indistinct indication of influence of *Joule* heat concentration in throat bottom Figure 5(d) may be seen in vertical cross-section  $x=0$ , where local maxima of instantaneous temperature near the surface of sediments “hill” are represented (Figure 5(e)), which are smaller in comparison with values in channel loop, – this temperature difference may reach  $\sim 35-65$  K depending on chosen flow time point.

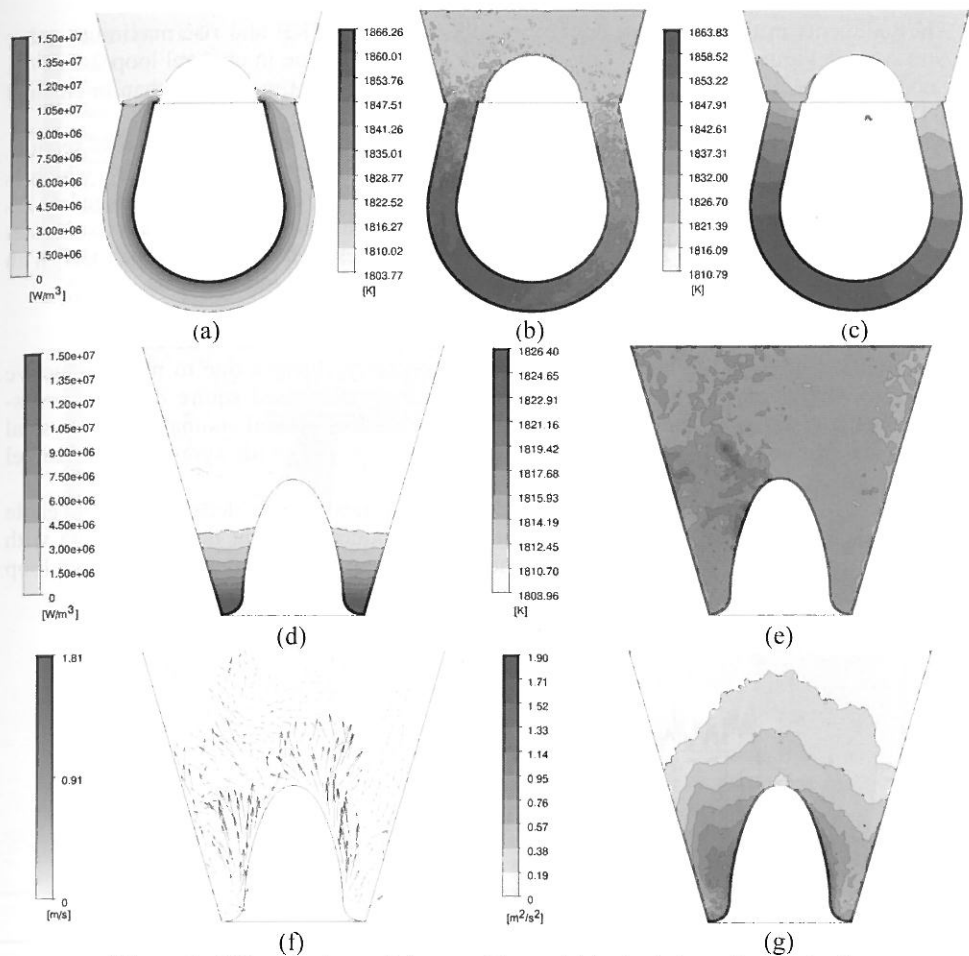


Figure 5. CIF with clogged throat – Figure 1(a). *Joule* heat density (a,d); instantaneous temperature (b,e) and velocity (f) fields obtained for flow time point  $t=41$  sec with LES turbulence model; time-averaged temperature (c) and turbulent kinetic energy (g) for flow time period  $t=27-41$  sec – cross-section  $y=0$  of channel loop and throat (a,b,c) and cross-section  $x=0$  of throat (d,e,f,g)

The time-averaged overheating temperature, which is determined as the difference between maxima of temperature in the channel and in the throat (Figure 5(c)), may be estimated as  $\Theta \sim 48\text{K}$  and this value is 1.5 times greater than in non-clogged CIF, where  $\Theta \sim 32\text{K}$  (Table 1). More precise value of overheating temperature may be obtained for longer period of time-averaging.

The absence of melt overheating in zone of *Joule* heat concentration near clogged throat bottom may be explained by noticeable changes of melt flow structure in the throat with intensive upstream with maximum velocity  $\sim 1.8$  m/s, which is represented in vertical cross-section  $x=0$  – Figure 5(f) (see also flow pattern in horizontal plane [5, Figure 3(d)]). To retrace the intensive melt flow in the throat of non-clogged CIF may be found above channel outlets [3, Figure 7(b)] with characteristic four-contour circulation in horizontal cross-section.

The sediments in throat bottom noticeably redistribute the TKE and rise maximum value  $\sim 1.9 \text{ m}^2/\text{s}^2$  (see Figure 5(g)), which is comparable with TKE value in channel loop  $2.1 \text{ m}^2/\text{s}^2$ . For non-clogged CIF the maximum of TKE in the throat is  $\sim 2.5$  times lower than in channel loop [3,4], where the intensive turbulent heat exchange is obtained.

As the melt is incompressible the transit velocity may be determined for any cross-section. The simplest way is to average for cross-section  $x=0$  the  $x$ -component of velocity, which is perpendicular to chosen transversal cross-section of the channel. The time-averaged (LES computed flow time period  $t = 27\text{--}41$  sec) transit velocity has prevailing direction to channel left outlet –  $v_{\text{trans}}^{\text{aver}} \sim -2$  cm/s (Table 1) – and this value corresponds to non-clogged CIF with  $\sim -2.8$  cm/s obtained for long-term time-averaging period (several minutes).

### ANOMALIES OF PHYSICAL FIELDS IN BUILD-UP CHANNEL MODEL

CIF model (Figure 1(b)), which represents the geometry changes due to non-conductive build-up formation in left channel branch with extremely decreased square of outlet cross-section till 25% in comparison with non-clogged branch, show several anomalies for physical fields in comparison with previously obtained results for CIF with symmetrical channel branches [3,4].

In zone of build-up of left channel branch the *Joule* heat power density has noticeable concentration (Figure 7(d)) due to drastic increase of induced current density (Eq. 1) with maximum value  $6.7 \cdot 10^7 \text{ W/m}^3$ , which is 4 times greater than maximum value in channel loop –  $1.62 \cdot 10^7 \text{ W/m}^3$  (Figure 7(a)), which corresponds to iron yoke position (Figure 1(b)).

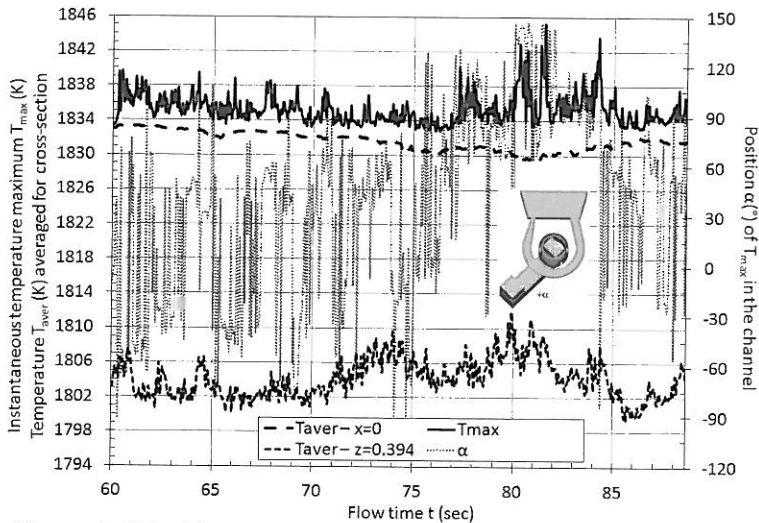


Figure 6. CIF with narrowed (25%) left channel branch – Figure 1(b).

Maximum of instantaneous temperature  $T_{\text{max}}$  (K) and angle  $\alpha$  ( $^\circ$ ) of its position at cross-section  $y = 0$ ; averaged for cross-sections  $x=0$  (bottom of channel loop) and  $z=0.394$  m (outlet of narrowed left channel branch to throat) temperature  $T_{\text{aver}}$  (K) – for flow time period  $t=60\text{--}88$  sec obtained with LES model of turbulence

The instantaneous temperature field has also two zones of competitive maxima values (Figures 7(b,e)) which correspond to zones of maxima of *Joule* heat power density. But similar zones are not obtained for temperature field, which is area-averaged for chosen cross-section. (Note that area-averaged field for chosen cross-section is time-dependent and than may be averaged by time.)

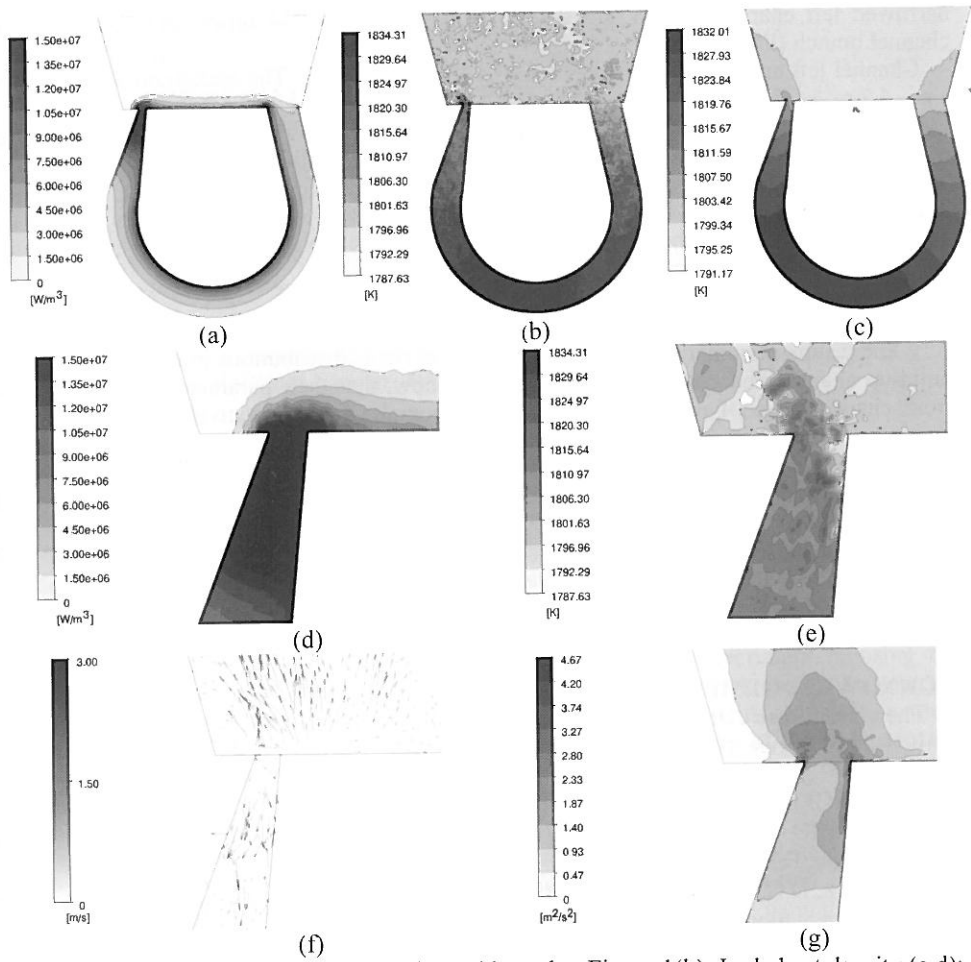


Figure 7. CIF with narrowed (25%) channel branch – Figure 1(b). Joule heat density (a,d); instantaneous temperature (b,e) and velocity (f) fields obtained for flow time point  $t=88$  sec with LES turbulence model; time-averaged temperature (c) and turbulent kinetic energy (g) for flow time period  $t=85-88$  sec – for cross-section  $y=0$  of channel loop and throat (a,b,c) and narrowed channel outlet (d,e,f,g)

Indeed, despite of maximum value of *Joule* heat power density in left channel outlet zone is 4 times greater than maximum value in channel loop (Figures 7(a,d)) the temperature averaged for cross-section of left channel outlet ( $z = 0.394$ ) is for  $\sim 30$ K smaller than temperature area-averaged for cross-section  $x=0$  (channel loop) – Figure 6.

The position of zone of time-averaged temperature maximum  $\sim 1832$ K is in the narrowed left channel branch –  $\alpha \sim 40^\circ$  (Figure 7(c)). The time-averaged overheating temperature may be estimated as  $\Theta \sim 37$ K and this value is for  $\sim 5$ K greater than one in non-clogged CIF (Table 1).

The absence of melt overheating zone in narrowed channel branch may be explained by extremely intensive melt flow near outlet to throat – maximum values of instantaneous velocity component (Figure 7(f)), which is perpendicular to the outlet cross-section of

narrowed left channel branch, are extremely larger (up to 2–4 times) than ones for right channel branch (Figure 3).

Channel left outlet is zone of prevailing generation of TKE. The maximum values of TKE are  $\sim 4.7 \text{ m}^2/\text{s}^2$  (Figure 7(g)).

The high levels of velocity values (up to  $\sim 3 \text{ m/s}$ ) produce extremely small values of area-averaged for cross-section transit velocity with rapid fluctuations in range  $\sim \pm 10 \text{ cm/s}$ . But time-averaged transit velocity has prevailing direction to narrowed left channel branch with build-up –  $v_{\text{trans}}^{\text{aver}} \sim -1 \text{ cm/s}$  (Table 1). As mentioned value of  $v_{\text{trans}}^{\text{aver}}$  is  $\sim 2.5$  times smaller than one in non-clogged CIF, the build-up of left channel branch may be considered as the cause of increased HD-resistance for transit flow.

## CONCLUSIONS

√ The results of numerical modelling of physical fields distributions in industrial CIFs with build-up channel and clogged bottom of throat show, that their parameters noticeable differ from characteristic of non-clogged CIF. The anomalies may negatively influence on CIF operation.

√ As anomaly of chosen field (e.g. *Joule* heat maxima) does not automatically indicate the cause of anomaly of another physical field (e.g. local overheating), for estimations of CIF clogging sequences it is necessary the application of complex analysis of physical fields.

√ Presented results of research show the effectiveness of LES study of industrial CIFs with geometry, which has been noticeably varied during operation period due to non-conductive build-up, clogging or erosion of ceramic lining and especially for CIFs with extremely narrowed channel branch.

## ACKNOWLEDGEMENTS

The current research was performed with the financial support of the ERAF project of the University of Latvia, contract No. 2011/0002/2DP/2.1.1.1.0/10/APIA/VIAA/085.

## REFERENCES

- [1] Drewek, R. (1996) *Verschleißmechanismen in Induktions-Rinnenöfen für Gußeisen und Aluminium*. Düsseldorf, VDI-Verlag.
- [2] Williams, D.C., Naro, R.L. (2007) Mechanism and control of buildup phenomenon in channel induction and pressure pouring furnaces. Part 1. *Ductile Iron News (Issue 1)*.
- [3] Baake, E., Jakovics, A., Pavlovs, S., Kirpo, M. (2010) Long-term computations of turbulent flow and temperature field in induction channel furnace with various channel design. *Magnetohydrodynamics*, 46, 317–330.
- [4] Baake, E., Jakovics, A., Pavlovs, S., Kirpo, M. (2011) Influence of the channel design on the heat and mass exchange of induction channel furnace. *The international journal for computation and mathematics in electrical and electronic engineering (COMPEL)*, 30, 1637–1650.
- [5] Jakovics, A., Pavlovs, S., Bosnyaks, D., Spitans, S., Baake, E., Nacke, B. (2012) Influence of channel and yoke design and clogging on turbulent flow and heat exchange in induction channel furnaces. *International Journal of Iron and Steel Research*, 19 (Supplement 1), 749–753.